AMERICAN ACADEMY OF OPHTHALMOLOGY®

Vortex Veins in Eyes With Pachychoroid Spectrum Disorders Evaluated by the Adjusted Reverse 3-Dimensional Projection Model

Ryoh Funatsu, MD,[1] Shozo Sonoda, MD, PhD,[1] Hiroto Terasaki, MD, PhD,[1] Hideki Shiihara, MD, PhD,[1] Mariko Hirokawa, ME,[2] Ji Yuanting, ME,[2] Yasushi Tanabe, ME,[2] Taiji Sakamoto, MD, PhD[1]

Purpose: To compare the distribution of vortex vein ampulla (VVA) between pachychoroid spectrum disorder (PSD) and controls.

Design: A single-center, case-control study.

Participants: This study included 75 PSD, 35 fellow, and 65 control eyes.

Methods: We quantified VVA distribution using a 3-dimensional reverse projection model corrected for image distortion. We investigated the distribution of major drainage veins (MDV), in which macular Haller's vessels directly influx.

Main Outcome Measures: The mean distances from the optic disc to VVAs and the mean angles between VVAs and the fovea-disc line.

Results: The PSD group had significantly fewer VVA in infranasal sector (PSD, fellow, control; 1.6 ± 0.6, 1.8 ± 0.6, 1.9 ± 0.6, respectively, $P = 0.026$). In supralateral sector, for PSD, fellows, and controls, the mean distances from the optic disc to VVAs were 14.1 ± 1.0 mm, 14.1 ± 1.1 mm, and 13.6 ± 1.4 mm, respectively, and were significantly farther in PSD than in controls ($P = 0.023$). The mean angles between VVAs and the fovea-disc line were 64.8 ± 5.9°, 66.4 ± 6.4°, and 61.7 ± 6.4°, respectively, and were significantly higher in PSD and fellows than in controls ($P = 0.008$). The mean distances from the optic disc to MDV in supratemporal sector were 14.1 ± 1.2 and 13.7 ± 1.2 in eyes whose Haller's vessels extended beyond the fovea-disc line (asymmetry), and those that did not, respectively, with the asymmetric eyes significantly farther ($P = 0.016$).

Conclusions: The VVA position in supralateral sector was farther and higher in PSD than in controls, suggesting that the distribution of VVA may be associated with the development of PSD.

Financial Disclosure(s): Proprietary or commercial disclosure may be found after the references. *Ophthalmology Science 2023;3:100320*

Supplemental material available at www.aaojournal.org.

Pachychoroid spectrum disorders (PSD) are the major diseases that present with exudative changes in the macula and can cause severe and irreversible visual impairment in the chronic phase.[1,2] The development of OCT allows noninvasive and detailed examination of the choroid, such as enhanced depth imaging OCT and en face imaging.[3,4] Choroidal thickening, dilated Haller's vessels, asymmetry of Haller's layer, and anastomosis of Haller's vessels at the watershed are characteristic of PSD, and abnormal choroidal circulation is believed to be involved in its pathophysiology.[3,5–11] The concept of venous overload choroidopathy was proposed as an umbrella concept for these diseases.[12] Recently, it has been reported that PSD presents dilatation of the vortex vein ampulla (VVA) and thickening of the anterior sclera,[13–17] suggesting that vortex vein (VV) congestion is involved in the pathogenesis of PSD. Vortex veins, the major drainage channels of the choroid[17] have attracted much attention, but little analysis has been conducted on the distribution of VV.

Indocyanine green angiography (ICGA) is the standard technique for evaluating choroidal vessels,[14,15,18] but it is relatively invasive and ethically problematic to perform in many healthy individuals.[19] Therefore, the information on peripheral choroidal vessels collected by ICGA is limited, and it is practically challenging to compare pachychoroidal images with normal ones, which have many variations.[20–22] Furthermore, when examining the location of peripheral choroidal vessels, it is difficult to capture the entire fundus even with an ultrawide-field fundus image. Distortion makes strict quantitative evaluation difficult even if a montage image is created.[20,21]

https://doi.org/10.1016/j.xops.2023.100320
ISSN 2666-9145/23

To solve these problems, we developed an adjusted 3-dimensional (3D) reverse projection model method to noninvasively quantify the peripheral choroid without dye by extracting choroidal vascular enhancement images from undistorted montaged ultrawide-field fundus images and reported the distribution of VVA in healthy subjects.[20,23] This technique enables an accurate and noninvasive analysis of VV locations. We hypothesized that choroidal vascular pathology in eyes with PSD is characteristic of VVA. Using the above technique, we quantitatively compared the positional information of the VVA between normal eyes and pachychoroid eyes to investigate the characteristics of PSD.

Methods

This was a single-center retrospective observational study. This study was approved by the Ethics Committee of Kagoshima University, Kagoshima, Japan (no. 16012). All procedures were performed in accordance with the tenets of the Declaration of Helsinki.

Subjects

The affected eyes of patients with $\geq$ 1 eye diagnosed with PSD who visited the Department of Ophthalmology at Kagoshima University Hospital between April 2018 and September 2021 were included, and we used the fellow eye and healthy eyes as controls. Images were obtained at the initial visit, and only treatment-naive eyes were included. The exclusion criteria were as follows: (1) aged $<$ 18 years; (2) axial length $>$ 27 mm; (3) history of internal ocular surgery other than external ocular surgery, pterygium surgery, cataract surgery, or laser iridectomy; (4) intraocular diseases other than PSD; and (5) blurred images. If both eyes had PSD, then the right eye was included. Based on previous reports, we excluded patients diagnosed with secondary central serous chorioretinopathy, such as steroid administration, collagen disease, current pregnancy, and Cushing's disease.[17] All participants underwent a general ophthalmic examination, including best-corrected visual acuity, intraocular pressure measurement, refraction test, axial length measurement, and assessment with slit-lamp biomicroscopy. Images were obtained as follows: (1) color fundus photography (DRI OCT Triton, Topcon); (2) swept-source OCT en face images (PLEX Elite9000, ZEISS); (3) multiple scanning laser fundus imaging (Optos California, Optos PLC); (4) ICGA and fluorescein angiography images (Optos California); and (5) enhanced depth imaging OCT (Spectralis HRA + OCT; Heidelberg Engineering). These examinations were performed by orthoptists, or physicians in charge.

Definition of PSDs

Diagnostic criteria for PSD were defined based on previous studies[1,9,24]: (1) presence of dilated outer choroidal vessels on OCT B-scan images, en face images, or ICGA; (2) choroidal vascular hyperpermeability in ICGA; and (3) no aggregated soft drusen. Patients (1), (2), and (3) were diagnosed with pachychoroid neovasculopathy when accompanied by choroidal neovascularization, pachychoroid pigment epitheliopathy when accompanied by retinal pigment epithelial abnormalities, and central serous chorioretinopathy when accompanied by serous retinal detachment and fluorescein angiography leakage point within the serous retinal detachment. The diagnosis was made upon discussion between 2 retina specialist examiners (R.F. and H.S.), and in case of different opinions, a third retina specialist examiner (S.S.) was consulted to decide.

Montage of Ultrawide-field Fundus Image

Noninvasive ultrawide-field fundus image emphasizing choroidal vasculature without dye has already been reported.[23] Moreover, the adjusted 3D reverse projection model method, which synthesizes the ultrawide-field fundus image and displays its positional information without distortion, has also been reported.[20] Briefly, using Optos California, 2 off-axis images were taken to capture the entire fundus area. Then, an on-axis image is used as a reference to obtain a montage image by merging the 2 off-axis images without misalignment using a geometric transformation. Subsequently, by the inverse-stereo projection of this montage image onto a 3D eye model adjustable by axial length, we can more accurately determine the positional information of VVAs according to the individual eye size from the 2D montage image.

Evaluation of the Distribution of VVA

The following decisions were made by 2 retina specialist examiners (R.F. and H.S.) with discussion, and in case of different decisions, a third retina specialist examiner (S.S.) will decide. Because VVA takes a pear-like shape in fundus photography, it is necessary to determine its reference point. Therefore, the center of gravity was determined based on our previous report and set as the reference point for each VVA.[20] The following outcomes were measured: (1) the number of VVA; (2) distance from the optic disc to the VVA; and (3) angle between the VVA and the straight line connecting the fovea and the optic disc (fovea-disc line) (Fig S1).

The montage image was divided into 4 quadrants using 2 boundaries based on the watershed of Haller's vessels.[25] Specifically, the fovea-disc line was used as the horizontal boundary, and the line orthogonal to the fovea-disc line on the optic disc was used as the vertical boundary (Fig 2). The fovea-disc line is 0° on the temporal side, the upper side of the straight line orthogonal to that line at the optic disc is 90°, and the lower side is −90°. The nasal side of the fovea-disc line was defined as 180°. If there are multiple VVAs in each region, the representative values of the region number, distance, and angle are the average values in that region.

VVA Receiving Perfusion From the Macula: Major Drainage Vein

Previous reports used the mean to evaluate the VVAs distribution in each quadrant,[20,22] but the choroidal blood flow in the macula mainly flows into a single VVA in each of the superior and inferior temporal quadrants (Fig 2). Therefore, there are 2 major drainage veins (MDVs) in each eye. The VVA that receives blood flow directly from the macula was defined as the MDV and was determined using the following method:

The VVAs, which are refluxing and collecting Haller's vessels running within a 3 mm radius of the fovea, were determined using OCT en face and ICGA images. Two examiners (R.F. and H.S.) performed this independently, and a third party (S.S.) decided whether the results differed. We examined the distance and angle of the MDV using the method described above.

Association Between the MDV and Choroidal Structure

The asymmetric running of Haller's vessels across the line connecting the optic disc and the fovea (fovea-disc line) and VV anastomosis are characteristic findings in patients with PSD.[10,26]

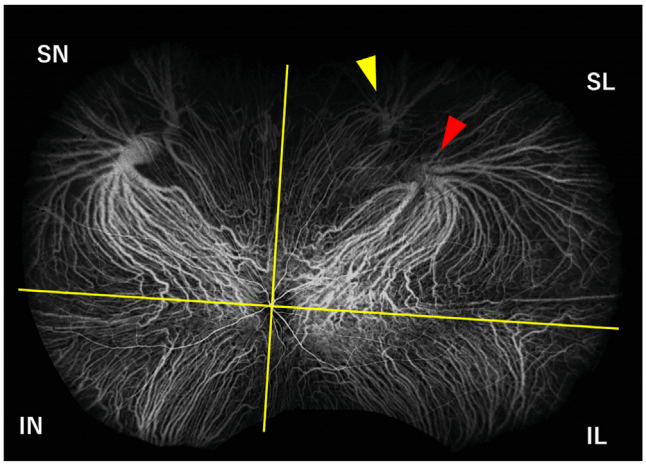

Figure 2. Ultrawide-field indocyanine angiography of eyes with pachychoroid spectrum disorder. We divided the ultrawide-field scanning laser ophthalmoscope image into 4 quadrants: supralateral (SL), infralateral (IL), supranasal (SN), and infranasal (IN) (yellow line), using the line connecting the fovea and the optic disc (fovea-disc line) and the line crossing it perpendicular to the optic disc as the borderline. The boundary is divided on a sphere but is shown in a planar view for convenience. By comparing the temporal (red arrowhead) and cephalic (yellow arrowhead) vortex veins in the SL sector, it is clear that almost all Haller's vessels in the macular region flow into the temporal vortex vein. The vortex vein on the temporal side was considered the major drainage vein.

Moreover, a previous report has shown that differences in ocular morphology correlate with the running patterns of Haller's vessels.[27] Using 12 × 12 mm OCT en face images, we defined symmetry types as those in which the upper and lower Haller's vessels run symmetrically across the fovea-disc line and asymmetry types as those in which either the upper or lower vessel exceeds the fovea-disc line. In addition, the presence of VV anastomosis was determined based on a previous report.[26] Decisions were made independently by retina specialist examiners (R.F. and H.S.) using a 12 × 12 mm OCT en face image, and a third retina specialist (S.S.) determined whether the results differed. Furthermore, we examined the associations between the MDV position and central choroidal thickness (CCT).

Statistical Analyses

Sex, age, axial length, spherical equivalent, best-corrected visual acuity, CCT, and running patterns of Haller's vessels were measured as patient backgrounds. We obtained the mean and standard deviation for continuous variables and the number and percentage for qualitative variables. The total number of VVAs per eye, total number of VVAs in each quadrant, and average distance and angle in each quadrant were calculated as representative values, and we report the overall mean and standard deviation for these values. For the MDV, 1 in the supralateral sector and 1 in the infralateral sector, the mean and standard deviation were calculated for the distance and angle. The Kruskal-Wallis test was used for continuous variables and Fisher exact test for qualitative variables to determine if there was any difference between PSD eyes, fellow eyes, and healthy eyes. Multiple comparisons were made using the Steel-Dwass test for the number, distance, and angle of the VVA that were statistically significant in the Kruskal-Wallis rank-sum test. The MDV of the PSD and healthy groups were compared and the significantly different characteristics between the 2 groups were examined. In addition, we analyzed the relationship between these characteristics and running patterns of Haller's vessels, VV anastomosis, and CCT. The R statistical software (version 4.0.5) was used for statistical analyses.[28] The R software packages used were as follows: ggplots2, viridis, dplyr, gtsummary, tidyverse, multcomp, ppcor, exactRankTests, irr, and NSM3.

Results

Demographics Data of the Participants

There were 75 eyes with PSD in 75 cases, 35 fellow eyes in 35 cases, and 65 control eyes in 65 cases, all Japanese (Table 1). For PSD, fellow, and control eyes, the ages were 56.1 ± 13.3, 51.1 ± 12.8, and 56.6 ± 17.8 years; male cases were 59 (79.0%), 29 (82.9%), and 43 (66.2%) eyes; and axial lengths were 23.68 ± 0.86 mm, 23.99 ± 0.79 mm, and 24.10 ± 1.41 mm, respectively, and there were no statistically significant differences (all $P \geq 0.103$, Table 1). Moreover, best-corrected visual acuities were 0.09 ± 0.26 logarithm of the minimum angle of resolution, −0.06 ± 0.14 logarithm of the minimum angle of resolution, and −0.01 ± 0.11 logarithm of the minimum angle of resolution, spherical equivalents were −0.27 ± 1.80 diopter, −0.99 ± 2.21 diopter, −1.51 ± 2.71 diopter, respectively, and there were statistically significant differences (all $P \leq 0.001$). The CCTs for PSD and fellow eyes were 375.8 ± 133.4 µm and 332.1 ± 133.9 µm, respectively, and for control eyes were 248.1 ± 111.9 µm and they were significantly different ($P < 0.001$). The number of eyes with VV anastomosis were 67 eyes (89.3%), 26 eyes (74.3%), and 33 eyes (56.9%) for PSD, fellow, and control eyes, respectively ($P < 0.001$). For PSD, fellow, and control eyes, the eyes with the symmetry type were 16 eyes (21.3%), 11 eyes (31.4%), and 36 eyes (62.1%), respectively. Furthermore, the eyes with the upper dominant Haller's vessel type were 31 eyes (41.3%), 15 eyes (42.9%), and 17 eyes (29.3%), and the eyes with the lower dominant Haller's vessel type were 28 eyes (37.3%), 9 eyes (25.7%), and 5 eyes (8.6%) for PSD, fellow, and control eyes, respectively ($P < 0.001$). Of the PSD eyes, 58 (77.3%) had a duration of > 6 months from onset. Cohen's kappa coefficients for the evaluations of the running pattern

Table 1. Background of Subjects With Pachychoroid-spectrum Disorders, Fellows, or Control Groups

Characteristics of Subjects	Pachychoroid-spectrum Disorders N = 75*	Fellow N = 35*	Control N = 65*	*P* Value†
Age (years)	56.1 ± 13.3	51.1 ± 12.8	56.5 ± 17.8	0.166
Sex (male)	59 (78.7%)	29 (82.9%)	43 (66.2%)	0.112
Type of disease				-
CSC	41 (54.7%)	-	-	
PPE	13 (17.3%)	-	-	
PNV	21 (28.0%)	-	-	
Spherical equivalent	−0.27 ± 1.80	−0.99 ± 2.21	−1.51 ± 2.71	0.001
Axial length (mm)	23.68 ± 0.86	23.99 ± 0.79	24.10 ± 1.41	0.103
The duration from the first episode (≥ 6 months)	58 (77.3%)	-	-	-
Central choroidal thickness (μm)	375.8 ± 133.4	332.1 ± 133.9	248.1 ± 111.9	< 0.001
The presence of vortex vein anastomosis	67 (89.3%)	26 (74.3%)	Data missing cases n = 7 (10.8%) 33 (56.9%)	< 0.001
The symmetry of Haller's vessel			Data missing cases n = 7 (10.8%)	< 0.001
Asymmetry	59 (78.7%)	24 (68.6%)	22 (37.9%)	
Symmetry	16 (21.3%)	11 (31.4%)	36 (62.1%)	
The running patterns of Haller's vessel			Data missing cases n = 7 (10.8%)	< 0.001
Upper	31 (41.3%)	15 (42.9%)	17 (29.3%)	
Lower	28 (37.3%)	9 (25.7%)	5 (8.6%)	
Symmetry	16 (21.3%)	11 (31.4%)	36 (62.1%)	
BCVA (logMAR)	0.09 ± 0.26	−0.06 ± 0.14	−0.01 ± 0.11	< 0.001

BCVA = best-corrected visual acuity; CSC = central serous chorioretinopathy; logMAR = logarithm of the minimum angle of resolution; PNV = pachychoroid neovasculopathy; PPE = pachychoroid pigment epitheliopathy.
*Mean ± standard deviation; n (%).
†Kruskal-Wallis rank sum test for continuous data; Fisher exact test for count data.

of Haller's vessels and VV anastomosis assessments were 0.712 and 0.556, respectively.

The Number of VVAs

The mean number of VVAs per eye was 7.6 ± 1.5, 7.9 ± 1.5, and 8.0 ± 1.3 for PSD, fellow, and controls, respectively, which were not significantly different ($P = 0.378$, Kruskal-Wallis rank-sum test, Table 2 and Fig S3). The mean number of VVAs in the infranasal sector was 1.6 ± 0.6, 1.8 ± 0.6, and 1.9 ± 0.6 for PSD, fellow, and controls, respectively, and was significantly higher in controls ($P = 0.026$, Table 2). The mean number of VVs in the supranasal, supratemporal, and infralateral sectors was not significantly different between the PSD, fellow, and control groups (all $P \geq 0.563$, Table 2). Multiple testing of the mean number of VVAs in the infranasal sector, which was statistically significant, between PSD, fellow, and controls showed significant differences only between PSD and controls (PSD vs. controls; $P = 0.019$, PSD vs. fellow; $P = 0.394$, fellow vs. controls; $P = 0.693$, Steel-Dwass test).

The Distance From the Optic Disc to the VVAs

The mean distances from the optic disc to the VVAs in the supralateral sector were 14.1 ± 1.0 mm, 14.1 ± 1.1 mm, and 13.6 ± 1.4 mm for PSD, fellow, and controls, respectively, and were significantly shorter in controls ($P = 0.018$, Table 2). Mean distances in the supranasal, infranasal, and infralateral sectors were not significantly different between PSD, fellow, and controls (all $P \geq 0.266$, Table 2). Multiple testing of the mean distance in the supralateral sector, which was statistically significant, between PSD, fellow, and controls showed significant differences only between PSD and controls (PSD vs. control; $P = 0.023$, PSD vs. fellow; $P = 0.997$, fellow vs. control; $P = 0.101$, Steel-Dwass test).

The Angle Between the VVAs and the Fovea-Disc Line

The mean angles between the VVAs and the fovea-disc line were 64.8 ± 5.9°, 66.4 ± 6.4°, and 61.7 ± 6.4° for PSD, fellow, and controls, respectively, and were significantly lower in controls ($P < 0.001$, Table 2). Mean angles in the supranasal, infranasal, and infralateral sectors were not significantly different between PSD patients, fellow patients, and controls (all $P \geq 0.072$, Table 2). Multiple testing of the mean angle in the supralateral sector, which was statistically significant, between PSD, fellow, and controls showed significant differences between PSD and control, and between fellow and controls (PSD vs. control; $P = 0.008$, PSD vs. fellow; $P = 0.534$, fellow vs. control; $P = 0.002$, Steel-Dwass test).

Table 2. Characteristics of the Distribution of VVs by Group

Characteristics of VV	Pachychoroid Disease N = 75*	Fellow N = 35*	Control N = 65*	*P* Value†
The number of VV				
Total	7.6 ± 1.5 (4–11)	7.9 ± 1.5 (6–12)	8.0 ± 1.3 (5–11)	0.378
Supranasal	2.1 ± 0.7 (1–4)	2.1 ± 0.6 (1–3)	2.2 ± 0.7 (1–4)	0.563
Supralateral	1.8 ± 0.7 (1–4)	1.8 ± 0.5 (1–3)	1.8 ± 0.6 (1–3)	0.935
Infralateral	2.1 ± 0.5 (1–4)	2.2 ± 0.6 (1–3)	2.1 ± 0.6 (1–4)	0.611
InfraNasal	1.6 ± 0.6 (1–3)	1.8 ± 0.6 (1–3)	1.9 ± 0.6 (1–3)	0.026
The distance: optic disc-VV (mm)				
Supranasal	13.2 ± 1.6 (9.8–15.9)	13.2 ± 1.2 (8.6–15.0)	12.9 ± 1.2 (10.4–16.0)	0.226
Supralateral	14.1 ± 1.0 (11.6–16.7)	14.1 ± 1.1 (12.0–16.3)	13.6 ± 1.4 (11.1–16.7)	0.018
Infralateral	14.8 ± 1.1 (12.6–17.7)	14.8 ± 1.2 (13.0–17.7)	14.8 ± 1.5 (12.0–18.9)	0.875
Infranasal	13.0 ± 1.1 (10.2–16.0)	12.9 ± 1.2 (10.9–115.7)	13.1 ± 1.4 (10.2–16.7)	0.799
The angle: fovea-optic disc-VV (°)				
Supranasal	128.9 ± 9.1 (105.0–146.0)	127.5 ± 8.5 (109.3–154.5)	125.0 ± 6.8 (105.9–138.5)	0.072
Supralateral	64.8 ± 5.9 (49.5–78.8)	66.4 ± 6.4 (51.5–83.5)	61.7 ± 6.4 (48.4–78.3)	< 0.001
Infralateral	−56.8 ± 6.4 (−72.4 to −43.7)	−58.9 ± 6.0 (−73.7 to −47.7)	−58.4 ± 5.8 (−73.1 to −45.7)	0.194
Infranasal	−120.6 ± 7.1 (−137.0 to −104.0)	−119.0 ± 7.6 (−135.0 to −104.0)	−121.3 ± 6.8 (−137.5 to −103.0)	0.313

VV = vortex vein.
*Mean ± standard deviation (min.–max.).
†Kruskal-Wallis rank sum test for continuous data.

MDV

The mean distances from the optic disc to the MDV in the supralateral sector were 14.2 ± 1.1 mm, 14.1 ± 1.1 mm, and 13.6 ± 1.4 mm for PSD, fellow, and controls, respectively, and were significantly shorter in controls ($P = 0.019$, Table 3 and Fig 4). On the infralateral side, the mean distances were 14.9 ± 1.3 mm, 15.0 ± 1.3 mm, and 14.8 ± 1.6 mm for PSD, fellow, and controls, respectively, and were not significantly different between them ($P = 0.870$, Table 3 and Fig 4). Multiple testing of the mean distance in the supralateral sector, which was statistically significant, between PSD, fellow, and controls showed significant differences only between PSD and controls (PSD vs. control; $P = 0.017$, PSD vs. fellow; $P = 0.963$, fellow vs. control; $P = 0.164$, Steel-Dwass test).

The mean angles between the MDV and the fovea-disc line in the supralateral sector were 57.8 ± 8.0°, 59.5 ± 7.1°, and 54.7 ± 8.2° for PSD, fellow, and controls, respectively, and were significantly shorter in controls ($P = 0.010$, Table 3 and Fig 4). On the infralateral side, the mean angles were −46.5 ± 7.2°, −48.6 ± 7.7°, and −48.2 ± 6.7° for PSD, fellow, and controls, respectively, and were not significantly different ($P = 0.371$, Table 3 and Fig 4). Multiple testing of the mean angle in the supralateral sector, which was statistically significant, between PSD, fellow, and controls showed a significant difference between fellow and control and a marginally significant difference between PSD and controls (PSD vs. control; $P = 0.068$, PSD vs. fellow; $P = 0.652$, fellow vs. control; $P = 0.011$, Steel-Dwass test).

Relationship Between MDV in the Supralateral Sector and the Running Patterns of Haller's Vessels

In this study, the MDV characteristics that differed significantly between the PSD, fellow, and control groups were the

Table 3. Characteristics of the Distribution of Main VVs by Group

Characteristics of Main VV	Pachychoroid Disease N = 75*	Fellow N = 35*	Control N = 65*	*P* Value†
The distance: optic disc-major VV (mm)				
Supralateral	14.2 ± 1.1 (11.6–17.2)	14.1 ± 1.1 (12.0–17.4)	13.6 ± 1.4 (11.1–16.8)	0.019
Infralateral	14.9 ± 1.3 (12.4–18.0)	15.0 ± 1.3 (13.2–18.2)	14.8 ± 1.6 (11.4–18.4)	0.870
The angle: fovea-optic disc-major VV (°)				
Supralateral	57.8 ± 8.0 (37.5–78.8)	59.5 ± 7.1 (47.3–83.5)	54.7 ± 8.2 (40.5–78.3)	0.010
Infralateral	−46.5 ± 7.2 (−62.1 to −32.2)	−48.6 ± 7.7 (−63.4 to −33.7)	−48.2 ± 6.7 (−66.2 to −32.9)	0.371

VV = vortex vein.
*Mean ± standard deviation (min.–max.).
†Kruskal-Wallis rank sum test for continuous data.

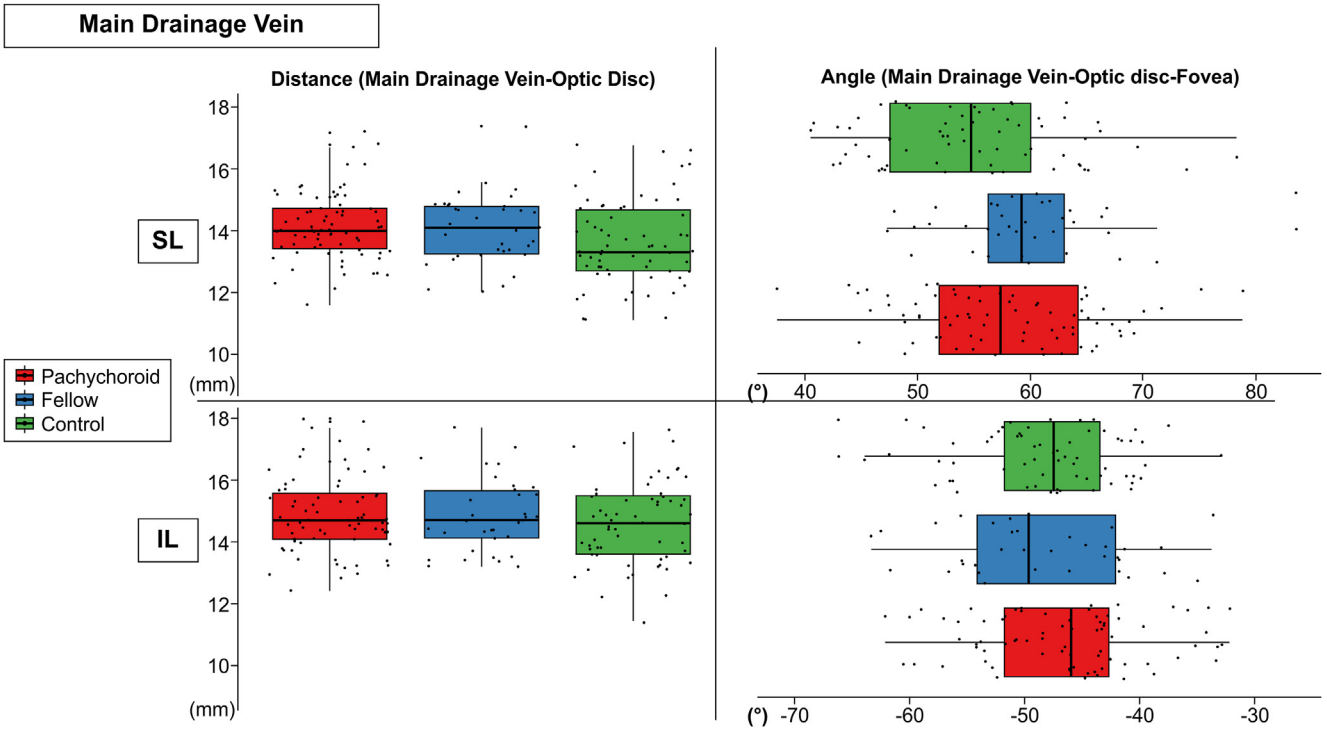

Figure 4. Box and whisker diagram for the average distance and angle of major drainage vein (MDV). Box and whisker diagram showing the distance from the optic disc to the MDV of each sector between the pachychoroid spectrum disorder (PSD), fellow, and healthy groups for each sector (PSD vs. fellow vs. control: the supralateral [SL] sector, 14.2 ± 1.1 mm vs. 14.1 ± 1.1 mm vs. 13.6 ± 1.4 mm, $P = 0.019$; the infralateral [IL] sector, 14.9 ± 1.3 mm vs. 15.0 ± 1.3 mm vs. 14.8 ± 1.6 mm, $P = 0.870$). Box and whisker diagram showing the angle between the fovea-disc line and the MDV of each sector between the PSD, fellow, and healthy groups for each sector (PSD vs. fellow vs. control: the SL sector, 57.8 ± 8.0° vs. 59.5 ± 7.1° vs. 54.7 ± 8.2°, $P = 0.010$; the IL sector, −46.5 ± 7.2° vs. −48.6 ± 7.7° vs. −48.2 ± 6.7°, $P = 0.371$).

distance from the optic disc to the MDV and the angle between the fovea-disc line and the MDV in the supralateral sector (Table 3). We examined the relationship between the characteristics of the MDV in the supralateral sector and the running patterns of Haller's vessels and CCT using a post hoc analysis.

Regarding the distance between the MDV and the optic disc, the asymmetric type was significantly longer than the symmetric type (asymmetry vs. symmetry, 14.1 ± 1.2 vs. 13.7 ± 1.2, $P = 0.016$, Mann−Whitney U test, Table 4 and Fig 5). Multiple tests of the mean distance in the supralateral sector showed a significant difference between the upper asymmetry group and the symmetry group (upper asymmetry vs. symmetry; $P = 0.015$, upper asymmetry vs. lower asymmetry; $P = 0.355$, lower asymmetry vs. symmetry; $P = 0.525$, Steel−Dwass test). However, the angle between the fovea-disc line and the MDV did not differ between the running patterns of Haller's vessels. For the infralateral MDV, the mean distance between the MDV and optic disc was longer in eyes with upper asymmetry group than that of eyes with the symmetric and lower asymmetry group ($P = 0.025$, Table 5). Multiple tests of the mean distance in the infralateral sector showed a significant difference between the upper asymmetry group and the symmetry group (upper asymmetry vs. symmetry; $P = 0.166$, upper asymmetry vs. lower asymmetry; $P = 0.026$, lower asymmetry vs. symmetry; $P = 0.543$, Steel-Dwass test).

There were no significant associations between CCT and the distance between the MDV and the optic disc, or between CCT and the angle between the fovea-disc line and the MDV in both the supralateral and infralateral sectors (All $P \geq 0.064$, Fig S6 and Table S6). In addition, there was no apparent association between the presence of VV anastomosis and the MDV position (All $P \geq 0.064$, Table S7).

Discussion

In this study, the VVAs in the supralateral sector were located farther from the optic disc in the PSD eyes than in the controls, and VVAs in the PSD eyes and the fellow eyes were located higher than in the controls (Fig 7). This was the case despite no significant difference in the axial length between the groups. Additionally, the distance should be longer for the controls because the axial length is relatively long, but the result is the opposite.

The mean angles between the VVAs and fovea-disc lines in the supralateral sector were significantly larger in the PSD and fellow eyes than in the controls. In other words, the VVAs were positioned higher in the eyes with PSD (Fig 7).

Table 4. Difference in the Distribution of the SL Major VV Between the Running Patterns of Haller's Vessels

Characteristics of SL Major VV	Distributions of Major VV			P Values[†]
Running patterns of Haller's vessel	Symmetry* n = 63	Asymmetry* n = 105	-	
The distance OD-SL major VV (mm)	13.7 ± 1.2 (11.1–17.4)	14.1 ± 1.2 (11.1–17.2)	-	0.016
The angle Fovea-OD-SL major VV (°)	57.1 ± 7.6 (42.9–78.3)	57.3 ± 8.4 (37.5–83.5)	-	0.936
Running patterns of Haller's vessel	Symmetry* n = 63	Asymmetry's direction: Upper* n = 63	Asymmetry's direction: Lower* n = 42	
The distance OD-SL major VV (mm)	13.7 ± 1.2 (11.1–17.4)	14.2 ± 1.1 (11.8–16.6)	13.9 ± 1.4 (11.1–17.2)	0.021
The angle Fovea-OD-SL major VV (°)	57.1 ± 7.6 (42.9–78.3)	55.8 ± 7.4 (40.5–78.8)	59.5 ± 9.3 (37.5–83.5)	0.678

OD = optic disc; SL = supuralateral; VV = vortex vein.
*Mean ± standard deviation (min.–max.).
[†]Kruskal-Wallis rank sum test and Mann-Whitney *U* test for continuous data.

In a report by Tomita et al using laser speckle flowgraphy in humans, the retinal blood flow was higher in the upper hemisphere than in the lower hemisphere. They mentioned that this difference may create a difference in reflux in the upper and lower retina and may be associated with the pathogenesis of central serous chorioretinopathy with asymmetrical choroidal vessels.[29] In the whole body, the lower organs are more prone to fluid stasis because they need to circulate blood against blood pressure.[30] For example, systemic venous overload in heart failure causes edema in the lower legs.[31] In other words, upward draining veins may be more prone to blood flow congestion than downward draining veins. The more distant and upper location of the supralateral VVA in PSD eyes in the present study suggests that they are structurally more prone to choroidal blood stasis than controls.

Furthermore, the distance to the MDV on the supralateral and infralateral side was associated with the running pattern of the Haller's vessels (Tables 4 and 5). In particular, the distance of the upper dominant Haller's vessels was significantly longer than that of the symmetrical type in the supralateral sector and longer than that of the lower asymmetry type in the infralateral sector (Figs S8 and S9). The present result, that the difference in the distance to the MDV may be associated with the running pattern of Haller's vessels, which is a risk factor for PSD, is consistent with the report that differences in ocular morphology are correlated with the Haller's vessels running pattern.[27] It is unclear how differences in the location of the major drainage channels contribute to the pathogenesis of PSD, but the following possibilities are considered. In the present study, we could quantitatively indicate that eyes in which the MDV on the supralateral side is farther from the optic disc have Haller's vessels that extend beyond the fovea-disc line. In these eyes, choroidal perfusion requires a greater force and may be prone to choroidal venous overload. This may be related to the fact that the choroid is thicker in the upper part than in the lower part.[32] Furthermore, the distance to the MDV in the supralateral sector was longer in the upper asymmetry

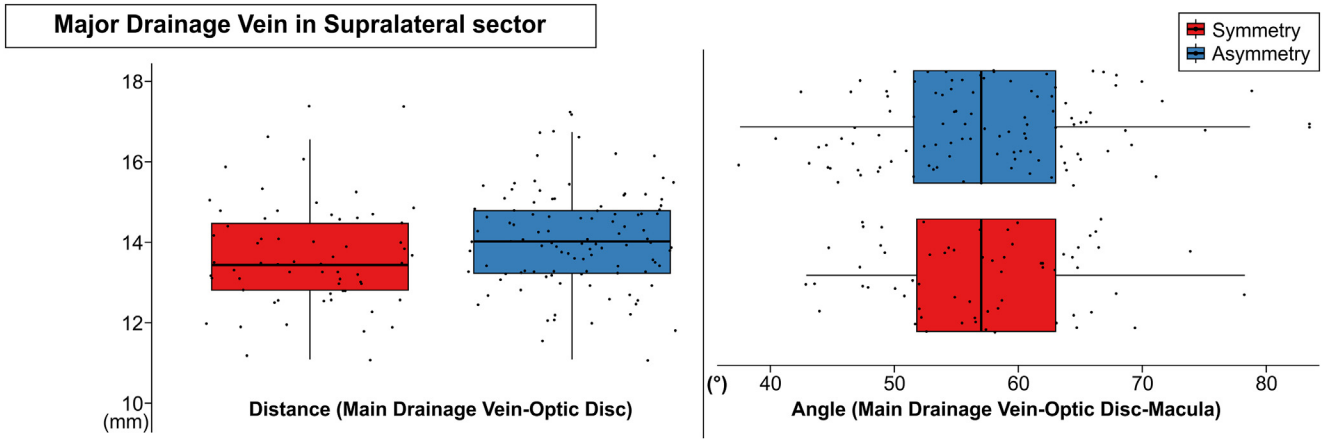

Figure 5. Box and whisker diagram for the average distance and angle of the major drainage veins (MDVs). Box and whisker diagram showing the average distance from the optic disc to the MDVs and the average angle between the fovea-disc line and the MDVs of the supralateral sector between the symmetric and asymmetric types (The distance, asymmetry vs. symmetry, 14.1 ± 1.2 mm vs. 13.7 ± 1.2 mm, $P = 0.016$; The angle, asymmetry vs. symmetry, 57.1 ± 7.6° vs. 57.3 ± 8.4°, $P = 0.936$).

Table 5. Difference in the Distribution of the IL Major VV Between the Running Patterns of Haller's Vessels

Characteristics of IL Major VV	Distributions of Major VV			*P* Values[†]
Running patterns of Haller's vessel	Symmetry* n = 63	Asymmetry* n = 105	-	
The distance OD-IL major VV (mm)	14.7 ± 1.4 (11.4–18.4)	14.9 ± 1.3 (12.3–18.2)	-	0.492
The angle Fovea-OD-IL major VV (°)	−46.4 ± 7.5 (−63.9 to −32.2)	−48.4 ± 7.0 (−66.2 to −33.4)	-	0.093
Running patterns of Haller's vessel	Symmetry* n = 63	Asymmetry's direction: Upper* n = 63	Asymmetry's direction: Lower* n = 42	
The distance OD-IL major VV (mm)	14.7 ± 1.4 (11.4–18.4)	15.1 ± 1.3 (12.9–18.2)	14.5 ± 1.3 (12.3–17.7)	0.025
The angle Fovea-OD-IL major VV (°)	−46.4 ± 7.5 (−63.9 to −32.2)	−48.0 ± 7.4 (−63.4 to −33.4)	−49.1 ± 6.5 (−66.2 to −39.3)	0.198

IL = infralateral; OD = optic disc; VV = vortex vein.
*Mean ± standard deviation (min.–max.).
[†]Kruskal-Wallis rank sum test and Mann-Whitney *U* test for continuous data.

type than in the lower asymmetry type, and the distance to the MDV in the infralateral sector was shorter in the lower asymmetry type than in the upper asymmetry type. Regarding the superior side, since the more distant position may require more force for choroidal perfusion due to the need to perfuse against gravity, this result may be related to the cause of the upper symmetry type and the malposition of MDV. For the inferior side, choroidal perfusion does not have to resist gravity. However, it is possible that eyes with a shorter distance to the MDV may have a smaller total vessel volume than eyes with a longer distance to the MDV, and the fluid may have a smaller capacity to accumulate. Therefore, since the eyes with pachychoroid have a higher resistance to choroidal blood outflow than normal eyes,[12,17] and blood tends to accumulate in the choroidal veins more easily, the lower asymmetric eyes with a shorter Haller's vessels may be more prone to result in overload due to choroidal fluid accumulation.

Of particular interest is that the angle of the VVA in the fellow eyes was similar to that of the PSD eyes and was located higher up from the fovea-disc line than in the normal eyes. This result suggests that there is a congenital predisposition for PSD since VV malposition is bilateral in patients with PSD. These findings are consistent with reports that genes related to choroidal vascular endothelium and vasculature growth are characteristic of patients with PSD[33,34] and that choroidal and scleral findings in fellow eyes with PSD are more similar to those in PSD eyes than in healthy eyes.[7,11,35,36] However, the sclera, which supports an outflow tract of the VV as well as the VVA, shows structural abnormalities in all areas,[17] in contrast to malposition of the VVA, which was observed only on the superior auricular side. As the cause of this regional difference is not clear from the present cross sectional study, future prospective studies on the development of VVA in childhood are needed. In addition, scleral thickness was not associated with the running patterns of

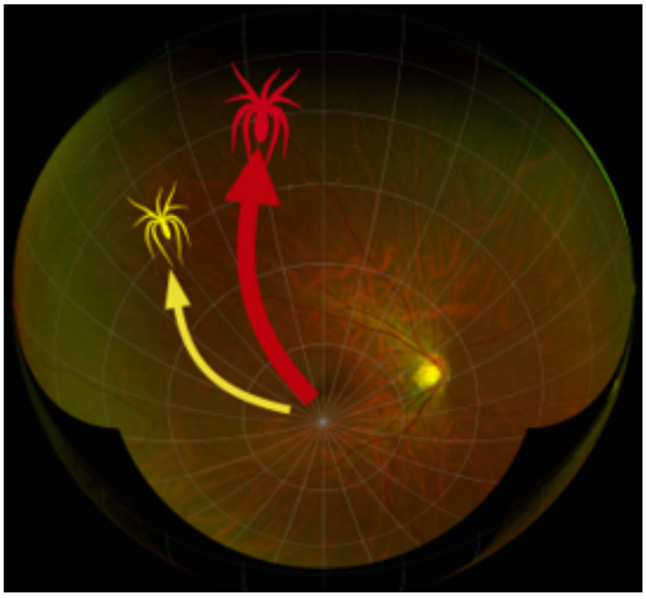

Figure 7. Schematic diagram for the displacement of the major drainage vein (MDV). Schematic diagram showing the displacement of the MDV on the supralateral side in an eye with pachychoroid spectrum disorder (PSD). In eyes with PSD, the MDV was located farther and upward from the optic disc.

Haller's vessels and was positively correlated with choroidal thickness,[27,37] whereas the malposition of the VVA was associated with the running patterns of Haller's vessels and not with choroidal thickness. Thus, the sclera and the VVA may have different relationships with the choroid. Moreover, the current results suggest that there is no apparent association between the presence of a VV anastomosis and the position of the MDV. At present, although it is unclear whether the interval from onset is related to VV anastomosis, 23.7% of all cases were acute type, and the presence of a certain number of acute type cases may be one of the reasons for the present results. However, because the details are unclear, the relationship between the occurrence of VV anastomosis and the location of MDVs should be prospectively investigated in future studies.

There was no difference in the total number of VV between the groups, but there were significantly fewer vortices on the inferior nasal side in PSD eyes (Table 2). The mean total VVA number was similar to that in previous reports, although it was relatively low only in eyes with PSD.[22,38] Vortex vein ampulla is the major drainage channel for choroidal blood flow, and its small number may increase blood flow to other drainage channels. Moreover, Bacci and Freund et al reported that eyes with PSD have a smaller infranasal VV area than normal eyes.[18] Pachychoroid spectrum disorder may present an increased choroidal circulatory load on the temporal side to compensate for the role of the nasal side, which has fewer drainage channels; however, more research is needed.[9,10]

This study has several limitations. This retrospective observational study was conducted in a single center with a small sample size. Furthermore, because all participants were Japanese, the external validity of the present results to other racial groups is unclear. We have reported the reliability, such as intraclass correlation coefficients of interrater, intrarater, and intrasubject, of the present method of measuring the location of the VVA; however, because the method is subjective, and reproducibility needs to be examined in further studies.[20] Another limitation of the present study was the subjective assessment of choroidal morphology. Although our study analyzed the location of the VVA, we did not evaluate the actual blood velocity or blood flow in the choroid; hence, it is unclear to what extent they were affected.[39] It would be necessary to compare the present results with those measured by laser speckle flowgraphy. Future studies should focus on the functional aspects of the eye and use the fovea as the reference point for analysis. In addition, central serous chorioretinopathy, a representative disease of PSD, has been reported to occur in myopic eyes. Since the present results were obtained in a population with an average spherical equivalent of emmetropia, it is unclear whether the results can be extrapolated to such eyes.

In conclusion, the VV in the supralateral sector were located farther up in the PSD eyes than in the normal eyes, but did not differ from the other VVAs. In addition, the small number of VVAs on the inferior nasal side suggests that other areas of the choroidal circulation may have been overloaded. Malposition of the VV may contribute to choroidal venous overload.

Acknowledgments

The authors thank the orthoptists Masatoshi Tomita, Kikuko Toyodome, and the staff at Kagoshima University Hospital for their support in the data collection process.

Footnotes and Disclosures

Originally received: December 24, 2022.
Final revision: April 13, 2023.
Accepted: April 17, 2023.
Available online: April 22, 2023. Manuscript no. XOPS-D-22-00268.

[1] Department of Ophthalmology, Kagoshima University Graduate School of Medical and Dental Sciences, Kagoshima, Japan.

[2] System Development Department, Nikon Corporation, Yokohama, Japan.

Disclosures:

All authors have completed and submitted the ICMJE disclosures form.

The authors have no proprietary or commercial interest in any materials discussed in this article.

This study was approved by the Ethics Committee of Kagoshima University, Kagoshima, Japan (no. 16012).

All research adhered to the tenets of the Declaration of Helsinki.

HUMAN SUBJECTS: This study was approved by the Ethics Committee of Kagoshima University, Kagoshima, Japan (no. 16012). All procedures were performed following the tenets of the Declaration of Helsinki. This study is based on a retrospective review of medical records and informed consent was not obtained.

Author Contributions:

Conception and design: Funatsu, Sonoda, Terasaki, Shiihara, Hirokawa, Yuanting, Tanabe, Sakamoto

Data acquisition and/or research execution: Funatsu, Sonoda, Terasaki, and Shiihara

Data analysis and/or interpretation: Funatsu, Sonoda, Terasaki, Shiihara, Hirokawa, Yuanting, Tanabe, and Sakamoto

Research design: Funatsu, Sonoda, Terasaki, Shiihara, Hirokawa, Yuanting, Tanabe, and Sakamoto

Obtained funding: Sakamoto (JSPS KAKENHI grant number 21H03095). Study was performed as part of the authors' regular employment duties.
Manuscript preparation: Funatsu, Sonoda, Terasaki, Shiihara, Hirokawa, Yuanting, Tanabe, and Sakamoto

Meeting presentation: The material has been presented at the 37th Annual Meeting of the Japanese Society for Ocular Circulation, Kyoto, Japan, September 24-26th 2021.

Abbreviations and Acronyms:
CCT = central choroidal thickness; **D** = dimensional; **ICGA** = indocyanine green angiography; **MDV** = major drainage vein; **PSD** = pachychoroid spectrum disorder; **VV** = vortex vein; **VVA** = vortex vein ampulla.

Keywords:
Vortex vein, Pachychoroid spectrum disorder, Central serous chorioretinopathy.

Correspondence:
Taiji Sakamoto, MD, PhD, Department of Ophthalmology, Kagoshima University Graduate School of Medical and Dental Sciences, Kagoshima, Japan. E-mail: tsakamot@m3.kufm.kagoshima-u.ac.jp.

References

1. Cheung CMG, Lee WK, Koizumi H, et al. Pachychoroid disease. *Eye (Lond)*. 2019;33:14−33.
2. Pang CE, Freund KB. Pachychoroid neovasculopathy. *Retina*. 2015;35:1−9.
3. Ferrara D, Mohler KJ, Waheed N, et al. En face enhanced-depth swept-source optical coherence tomography features of chronic central serous chorioretinopathy. *Ophthalmology*. 2014;121:719−726.
4. Spaide RF, Koizumi H, Pozzoni MC. Enhanced depth imaging spectral-domain optical coherence tomography. *Am J Ophthalmol*. 2008;146:496−500.
5. Dansingani KK, Balaratnasingam C, Naysan J, Freund KB. En face imaging of pachychoroid spectrum disorders with swept-source optical coherence tomography. *Retina*. 2016;36:499−516.
6. Lee WK, Baek J, Dansingani KK, et al. Choroidal morphology in eyes with polypoidal choroidal vasculopathy and normal or subnormal subfoveal choroidal thickness. *Retina*. 2016;36 Suppl 1:S73−S82.
7. Yang L, Jonas JB, Wei W. Choroidal vessel diameter in central serous chorioretinopathy. *Acta Ophthalmol*. 2013;91:e358−e362.
8. Baek J, Kook L, Lee WK. Choriocapillaris flow impairments in association with pachyvessel in early stages of pachychoroid. *Sci Rep*. 2019;9:5565.
9. Matsumoto H, Kishi S, Mukai R, Akiyama H. Remodeling of macular vortex veins in pachychoroid neovasculopathy. *Sci Rep*. 2019;9:14689.
10. Spaide RF, Ledesma-Gil G, Gemmy Cheung CM. Intervortex venous anastomosis in pachychoroid-related disorders. *Retina*. 2021;41:997−1004.
11. Shiihara H, Sonoda S, Terasaki H, et al. Quantitative analyses of diameter and running pattern of choroidal vessels in central serous chorioretinopathy by en face images. *Sci Rep*. 2020;10:9591.
12. Spaide RF, Gemmy Cheung CM, Matsumoto H, et al. Venous overload choroidopathy: a hypothetical framework for central serous chorioretinopathy and allied disorders. *Prog Retin Eye Res*. 2022;86:100973.
13. Pang CE, Shah VP, Sarraf D, Freund KB. Ultra-widefield imaging with autofluorescence and indocyanine green angiography in central serous chorioretinopathy. *Am J Ophthalmol*. 2014;158:362−371.e2.
14. Lee A, Ra H, Baek J. Choroidal vascular densities of macular disease on ultra-widefield indocyanine green angiography. *Graefes Arch Clin Exp Ophthalmol*. 2020;258:1921−1929.
15. Ryu G, Moon C, van Hemert J, Sagong M. Quantitative analysis of choroidal vasculature in polypoidal choroidal vasculopathy using ultra-widefield indocyanine green angiography. *Sci Rep*. 2020;10:18272.
16. Fernández-Vigo JI, Moreno-Morillo FJ, Shi H, et al. Assessment of the anterior scleral thickness in central serous chorioretinopathy patients by optical coherence tomography. *Jpn J Ophthalmol*. 2021;65:769−776.
17. Imanaga N, Terao N, Nakamine S, et al. Scleral thickness in central serous chorioretinopathy. *Ophthalmol Retina*. 2021;5:285−291.
18. Bacci T, Oh DJ, Singer M, et al. Ultra-widefield indocyanine green angiography reveals patterns of choroidal venous insufficiency influencing pachychoroid disease. *Invest Ophthalmol Vis Sci*. 2022;63:17.
19. Fineman MS, Maguire JI, Fineman SW, Benson WE. Safety of indocyanine green angiography during pregnancy: a survey of the retina, macula, and vitreous societies. *Arch Ophthalmol*. 2001;119:353−355.
20. Funatsu R, Terasaki H, Shiihara H, et al. Quantitative evaluations of vortex vein ampullae by adjusted 3D reverse projection model of ultra-widefield fundus images. *Sci Rep*. 2021;11:8916.
21. Mori K, Gehlbach PL, Yoneya S, Shimizu K. Asymmetry of choroidal venous vascular patterns in the human eye. *Ophthalmology*. 2004;111:507−512.
22. Verma A, Maram J, Alagorie AR, et al. Distribution and location of vortex vein ampullae in healthy human eyes as assessed by ultra-widefield indocyanine green angiography. *Ophthalmol Retina*. 2020;4:530−534.
23. Kakiuchi N, Sonoda S, Terasaki H, et al. Choroidal vasculature from ultra-widefield images without contrast dye and its application to Vogt-Koyanagi-Harada disease. *Ophthalmol Retina*. 2019;3:161−169.
24. Siedlecki J, Schworm B, Priglinger SG. The pachychoroid disease spectrum-and the need for a uniform classification system. *Ophthalmol Retina*. 2019;3:1013−1015.
25. Hayreh SS, Baines JA. Occlusion of the vortex veins. An experimental study. *Br J Ophthalmol*. 1973;57:217−238.
26. Matsumoto H, Hoshino J, Mukai R, et al. Vortex vein anastomosis at the watershed in pachychoroid spectrum diseases. *Ophthalmol Retina*. 2020;4:938−945.
27. Terao N, Imanaga N, Wakugawa S, et al. Short axial length is related to asymmetric vortex veins in central serous chorioretinopathy. *Ophthalmol Sci*. 2021;1:100071.
28. R Core Team. *R: A Language and Environment for Statistical Computing*. Vienna, Austria: R Foundation for Statistical Computing; 2021.
29. Tomita R, Iwase T, Ueno Y, et al. Differences in blood flow between superior and inferior retinal hemispheres. *Invest Ophthalmol Vis Sci*. 2020;61:27.
30. Hayreh SS, Edwards J. Ophthalmic arterial and venous pressures. Effects of acute intracranial hypertension. *Br J Ophthalmol*. 1971;55:649−663.
31. Philipson H, Ekman I, Forslund HB, et al. Salt and fluid restriction is effective in patients with chronic heart failure. *Eur J Heart Fail*. 2013;15:1304−1310.
32. Kakiuchi N, Terasaki H, Sonoda S, et al. Regional differences of choroidal structure determined by wide-field optical coherence tomography. *Invest Ophthalmol Vis Sci*. 2019;60:2614−2622.
33. Hosoda Y, Yoshikawa M, Miyake M, et al. CFH and VIPR2 as susceptibility loci in choroidal thickness and pachychoroid disease central serous chorioretinopathy. *Proc Natl Acad Sci U S A*. 2018;115:6261−6266.
34. Hosoda Y, Miyake M, Schellevis RL, et al. Genome-wide association analyses identify two susceptibility loci for

pachychoroid disease central serous chorioretinopathy. *Commun Biol*. 2019;2:468.
35. Moon H, Lee DY, Nam DH. Axial length in unilateral idiopathic central serous chorioretinopathy. *Int J Ophthalmol*. 2016;9:717−720.
36. Oh JH, Oh J, Togloom A, et al. Biometric characteristics of eyes with central serous chorioretinopathy. *Invest Ophthalmol Vis Sci*. 2014;55:1502−1508.
37. Imanaga N, Terao N, Sonoda S, et al. Relationship between scleral thickness and choroidal structure in central serous chorioretinopathy. *Invest Ophthalmol Vis Sci*. 2023;64:16.
38. Rutnin U. Fundus appearance in normal eyes. I. The choroid. *Am J Ophthalmol*. 1967;64:821−839.
39. Sugiyama T, Araie M, Riva CE, et al. Use of laser speckle flowgraphy in ocular blood flow research. *Acta Ophthalmol*. 2010;88:723−729.